Fashionable epoxy/clay nanocomposites using modified clay-loaded methyl blue dye

Nazeeha S. Alkayal[1], Sobhy E. Elsilk[2,3], Abeer S. Elsherbiny[4*] and Nehal A. Salahuddin[4]

Abstract

In this work, the elimination of methyl blue (MB) acidic dye from an aqueous solution was investigated using two types of modified montmorillonite. One was modified with dimethyl benzyl hydrogenated tallow ammonium chloride which was named claytone (APA). The other montmorillonite is modified with poly oxy propylene diamine (Jeffamine D-2000) and was referred to as clayD2000. The adsorption efficiency of claytone and clay D2000 was 1.4 mg/g at pH 2 and 1.4 mg/g at pH 6, respectively, after 60 min. Pseudo-second-order was the best model to explain the adsorption process for both surfaces. The maximum adsorption capacity, q_{max} according to Langmuir isotherm was 2.75 mg/g and 2.56 mg/g for claytone and clayD2000, respectively. The adsorption of MB on claytone was endothermic and exothermic for the adsorption on clayD2000. Additionally, the adsorption of MB on claytone was a favorable process and the uptake of MB on clayD2000 was favorable only at lower temperatures. A new approach was applied to valorize the colored loaded clays with MB dyes through the incorporation of the two products (MB/claytone and MB/clayD2000) into epoxy resin to fabricate colored epoxy nanocomposites that are stylish. The obtained nanocomposites were characterized using several techniques. The results of transmission electron microscopy (TEM) showed that the clay-loaded MB dye nanosheets were well distributed in the epoxy matrix. Thermal gravimetric analysis (TGA) exhibited that the epoxy/MB/clay nanocomposites were thermally stable compared with that of bare epoxy resin. The Vickers hardness test indicates that the hardness of the epoxy/MB/clay nanocomposites was significantly improved despite the addition of a minor amount of modified clay-loaded MB dye in comparison with unmodified epoxy resin. Moreover, the antimicrobial activity of the obtained nanocomposites has been tested against several types of bacteria and yeast. This study reveals the ability to use the solid wastes which are resulted from wastewater treatment for enhancing the properties of the epoxy polymer to suit various industrial requirements.

Keywords Epoxy resin, Modified-clay/MB, Nanocomposite, Thermal and hardness properties, Adsorption, Montmorillonite

Introduction

Contamination is a serious issue that is likely to get worse in the next years due to toxic and dangerous materials, colors, and pigments [24, 26, 36]. There are numerous kinds of organic dyes such as cationic (basic) dyes, mordant dyes, disperse dyes, metal-related dyes, reactive dyes, and anionic (acid) that are used in the industries of electroplating, textile, paper and solar cell [27]. For living beings, a lot of health risks can be caused due to the discharged dyes into the water system without sufficient purification. The chemicals of dyes cause some respiratory issues, allergic reactions in contact with the skin

*Correspondence:
Abeer S. Elsherbiny
abeer.elsherbiny@science.tanta.edu.eg
[1] Chemistry Department, Faculty of Science, King AbduAziz University, Jeddah 21589, Saudi Arabia
[2] Botany Department, Faculty of Science, Tanta University, Tanta 31527, Egypt
[3] Biological Science Department, Rabigh College of Science and Arts, King Abdulaziz University, Rabigh, 21911, Saudi Arabia
[4] Chemistry Department, Faculty of Science, Tanta University, Tanta 31527, Egypt

Alkayal *et al. Environmental Sciences Europe*   (2023) 35:45

Page 2 of 11

such as itching, irritations and dermatitis and numerous health defects. Azo dyes and aromatic amines produced from the degradation of these dyes are considered carcinogenic and highly toxic [4]. According to the persistence of the azo group, a big risk in the environment will be assumed due to the bioaccumulation of azo dyes [16]. As a result, it is important to reduce the eco-toxic effect as well as the potential risk to human health (Bustos et al. [28]) by removing these dyes from industrial wastes. As an example, the mutagenic effects of methyl blue (MB) were reported to be dangerous to human beings [12, 37].

Today, various methods of removing contaminants from water have been used [13, 22, 41, 49, 52]. Adsorption is a superior and extensively used approach among these technologies because of its low cost, ease of operation, and lack of toxic secondary products [1, 32, 42]. The use of effective adsorbents is critical for ensuring the efficacy of water treatment when using the adsorption approach [19, 21]. Clay minerals consider inexpensive and eco-friendly materials that have silicate layers with a thickness of around one nanometer [54]. Most clays consist of octahedral and tetrahedral layers which are placed in various ways. Sodium Montmorillonite (Na$^+$-Mt) is an example of a 2:1 clay mineral that consisted of two tetrahedral SiO_2 sheets that have an octahedral Al_2O_3 sheet between these sheets [2, 3]. Due to the net negative surface charge of Montmorillonite (Mt), it has been used as an adsorbent for the removal of cationic pollutants [2, 3, 54]. To use Mt as an adsorbent for anionic pollutants in water, or soil, the properties of Mt must improve by modifying its surface. There are many approaches had been applied to modify Mt [7]. As an example, the most common method is an ion exchange with organic ammonium cations [8]. However, the adsorption technique for removing dyes still has an apparent disadvantage, it does not lead to the degradation of the organic dyes in the end. In the previous works [5, 9, 10, 19, 25, 38] the wastewater purification process is completed after adsorption. The problem of how to deal with the surfaces that have adsorbed the dyes remains a significant one. Epoxy thermosets are an important class of polymers because they are versatile and have many applications. They can be used as matrices for fiber-reinforced composites, electric encapsulates, fiber-optic sheathing, adhesives, and coatings. However, because of their elevated degree of crosslinking, they are naturally brittle and vulnerable to damage, limiting their use in aerospace, automotive, and advanced electric purposes. [51]. Furthermore, their very little thermal and electrical conductivities severely restrict their use in functions that need efficient heat and static electricity dissipation. [18, 44]. These problems can be solved by modifying epoxy resin with various additives or fillers. Besides that, most industries prefer epoxy

coating to have higher density and viscosity with excellent thermal stability and adhesive property to protect against ultraviolet (UV) radiation [30, 31]. Different attempts have been taken to improve the strength, adhesiveness, and thermal stability of polymers using various types of reinforcing agents, such as glass fibers, graphene, silica, zinc oxide, iron, copper, cobalt, titanium oxide, etc. [29, 30, 30, 31, 31, 35]. The properties of the final products depend on the specific function of the fillers. The inorganic fillers improve the chemical resistance, mechanical, thermal, and electrical properties of the epoxy [17, 45]. Ho et al. [15] and Wang et al. [20]) enhanced the mechanical properties of epoxy using several percentages of nano-clay.

The present paper describes firstly, the adsorption performance of methyl blue (MB) dye from wastewater on organophilic montmorillonite (claytone) as well as on modified sodium montmorillonite with poly oxy propylene diamine (Jeffamine D-2000). Then the two loaded clays with MB dye have been incorporated into epoxy resin through in-situ polymerization to obtain new colored epoxy/MB/clay nanocomposites. The obtained epoxy/MB/clay nanocomposites were characterized using X-ray diffraction (XRD) and Transmission electron microscope (TEM). The thermal stability and hardness of the new epoxy nanocomposites will be examined. Additionally, the antimicrobial activity of the prepared epoxy nanocomposites was studied. This approach opens the door to preparing colored reinforced polymer nanocomposites by reusing adsorbents that have already adsorbed organic dyes from wastewater. Moreover, improve the properties of the epoxy polymer to suit various industrial requirements. That is will give up a new path to effectively treat wastewater on a large scale by adsorption process and using the solid wastes for improving the thermal and mechanical properties of polymeric materials to fit several industrial applications.

Experimental
Materials
All of the reagents are commercially accessible, and no additional purification was performed before the reactions. Two types of modified clay minerals were utilized in this study. The first one was organophilic montmorillonite from southern clay products Inc (Gonzales, Texas, USA) under the market name claytone APA. The d_{001} interlayer spacing is 18.4 Å. The organically modified silicate was produced through a cation exchange reaction between the silicate and dimethyl benzyl hydrogenated tallow ammonium chloride. The organic content (dimethyl benzyl hydrogenated tallow ammonium chloride) was 24%. The second type was named clay D2000 and obtained from our prior work [40]. Epoxy resin of average

Alkayal *et al. Environmental Sciences Europe*   (2023) 35:45

Page 3 of 11

molecular weight 340.41 g/mol, 1,2-diaminopropane (curing agent), dichlorodimethylsilane and methyl blue dye were purchased from Sigma–Aldrich.

Adsorption study

Adsorption experiments were conducted separately for each type of clay in a batch method. In these experiments, 5 mL of claytone aqueous suspension (2 g/L) and 3 mL of MB dye solution (239.5 mg/L) at pH = 2 of phosphate buffer was shaken in Erlenmeyer flasks ((Julabo D-7633 Seelbach, Germany) for a particular period at 120 rpm and 25 ± 0.2 ℃. The adsorbent was separated using (Centrifuge-BL II Selecta) after a specific time, and the amount of MB contained in the aqueous solution was determined using a UV–visible spectrophotometer. (SPECORD 210 PLUS spectrophotometer) at $\lambda_{max} = 605$ nm. The adsorption capacity q_e, was estimated from the mass balance Eq. (1):

$$q_e = (C_o - C_e)V/m \qquad (1)$$

where, C_o and C_e denote the initial and equilibrium concentrations (mg/L) of MB, respectively, V denotes the volume (mL) of MB solution, and m denotes the mass (g) of the adsorbent utilized.

The adsorption kinetics was investigated by measuring adsorption capacities at various periods. Adsorption isotherms were determined by incubating MB solutions with adsorbents at 25 ± 0.2 ℃ until the equilibrium was reached. The impact of temperature was studied at temperatures 25, 35, and 45 ℃ ± 0.2 ℃, respectively. All assays were completed in duplicate, and the average values were calculated. The adsorption experiment of MB on clayD2000 and the adsorption capacity, q_e, were similarly measured at a neutral medium. After centrifugal separation at 6000 rpm for 10 min, the loaded clays with MB were collected and dried at 60 ℃ under vacuum to produce MB/clayD2000 and MB/claytone.

Preparation of epoxy resin

The ratio of epoxy/1,2-diaminopropane was 87.33:12.67 by weight. Consequently, 4.08 g of epoxy was mixed with 0.592 g of 1,2-diaminopropane and stirred under vacuum for 20 min at 25 ℃. The mixture was poured into a glass mold which was pretreated by dichlorodimethylsilane, followed by curing in an oven at 80 ℃ for 2 h then at 120 ℃ for 3 h.

Fabrication of epoxy/loaded methyl blue dye/clay nanocomposites

Two modifiers were used, dimethyl benzyl hydrogenated tallow ammonium chloride and poly oxy propylene diamine (Jeffamine D-2000) having an average molecular weight of 2000 g/mol and primary amine content of

0.97 meq/g, Fig. 1. The composites were performed by a simple solvent mixing method. A certain amount of MB/clayD2000 (or) MB/claytone was dispersed in epoxy in a round flask for 20 min using sonication at 25 ℃. Then, 1,2-diaminopropane was added to the mixture with stirring under a vacuum for 20 min at 25 ℃. The mixture was poured into a glass mold which was pretreated with dichlorodimethylsilane. Then curing was done in the oven at 80 ℃ for 2 h followed by 3 h at 120 ℃. In each system, the ratio of loaded clay/epoxy was 7.5/92.5 by weight.

Characterization

To investigate the prepared samples of epoxy, epoxy/MB/claytone and epoxy/MB/clayD2000, X-ray diffraction (XRD) was performed on Philips PW1710 equipped with Cu Kα tube which is a source of high-intensity radiation (λ = 1.5418 Å) (Germany). The sample was subjected to the range of 2θ = 3° to 20° with a scan rate of 8 (deg/min) at room temperature. Transmission electron microscope (TEM) specimens were cut from nanocomposites block using an ultra-microtome, LEICA EM UC6 equipped with a glass knife. By sliding the sample across a knife edge, the ultra-thin films (40–50 nm) were cut and then placed on copper grids at room temperature. TEM images were captured with a JEOL JEM-2100 Electron Microscope (Japan). Perkin Elmer thermogravimetric analyzer TGA4000 (France) under airflow of 25 mL min^{-1} was used to perform the thermogravimetric analysis (TGA). The samples (5–10 mg) were heated from room temperature to 800 ℃ at a linear heating rate 20 ℃ min^{-1}. The microhardness was measured using Zwick/Roell Indentec machine. 300 g were applied for 20 s in a perpendicular direction during the hardness test. Five readings were obtained for each data point, and the average value was computed.

Antimicrobial activity of the prepared nanocomposites

Escherichia coli, Bacillus subtilis, Staphylococcus aureus, Salmonella typhimurium, Klebsiella pneumoniae, Pseudomonas aeruginosa, and *Candida albicans* were taken
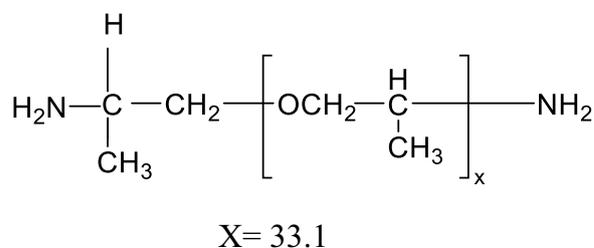

X= 33.1

Fig. 1 Chemical structure of Jeffamine D2000

Alkayal *et al. Environmental Sciences Europe*   (2023) 35:45

Page 4 of 11

from the Bacteriology Unit's culture collection at the Botany Department of the Faculty of Science at Tanta University for use in the experiment. The test bacteria and yeast-like fungus were grown on nutrient agar and Sabouraud's broth. The cut plug method (Anderson et al. [33]) was used to assess the antibacterial activity of epoxy, epoxy/MB/claytone, and epoxy/MB/clayD2000 on plates containing the test bacteria and inoculum fungus. Inoculums were diluted to 1×10^5 cfu/mL and overnight cultures of the bacterial and *C. albicans* indicators were prepared in nutrient and sabouraud broths. 200 mL of 1×10^5 cfu/mL were thoroughly mixed. Following solidification, 5 mm diameter wells were created, and each was filled with 0.2 gm of the tested nanocomposites (tested nanocomposites are not dissolved in any solvent). The widths of the inhibition zones were then measured to determine the inhibitory effects after the plates had been incubated at 30 °C for 24 h.

Results and discussion

The organically modified montmorillonite renders the hydrophilic character of montmorillonite and increases its organophilic nature leading to improving its swelling in organic solvents and its wetting properties with epoxy resin. In addition, the adsorption of organic dyes onto the modified clay facilitates the migration of hardener and epoxy into clay layers. Upon curing the epoxy reacts with hardener (1,2-diaminopropane) leading to the formation of epoxy/modified clay-loaded dye nanocomposite.

Adsorption studies
Effect of pH

In the adsorption process, the pH of the dye solution has a key role in the adsorption capacity determination. This is due to its impact on the adsorbent's surface characteristics as well as the ionic form of the adsorbate. Therefore, pH experiments of the adsorption of MB onto claytone and clalyD2000 were examined in the pH range of 2–6 using phosphate buffer. Figure 2 displays the equilibrium adsorption capacity of MB onto claytone and clayD2000 in a water solution with various pH values. The experiments were done in the pH range of 2–6 because the color of the MB solution fades at pH > 6 [14]. With an initial concentration of MB of 239.94 mg/L, it could be noted that the adsorption capacity raised from 0.570 mg/g to 0.742 mg/g with the acidity increased for claytone. Because MB is an ionic dye, the increased adsorption capacity could be due to the increased electrostatic interaction between MB and the claytone surface. However, an increment in the adsorption capacity of clayD2000 was found from 0.063 mg/g to 0.628 mg/g as the medium becomes neutral (pH = 6).
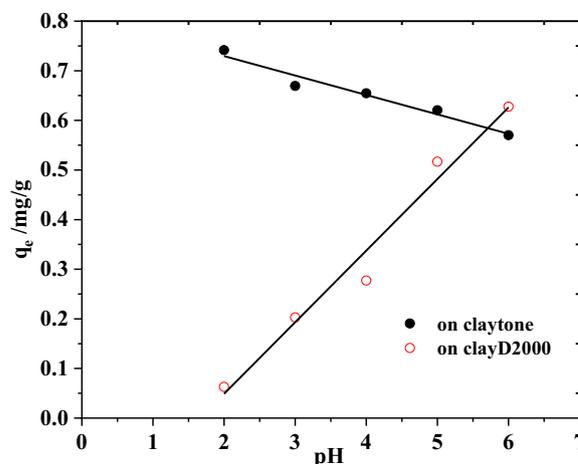

Fig. 2 Effect of initial pH of the medium on the adsorption capacity of MB onto claytone and clay D2000 (2 g/L) at 25 °C, $[MB]_0 = 239.5$ mg/L
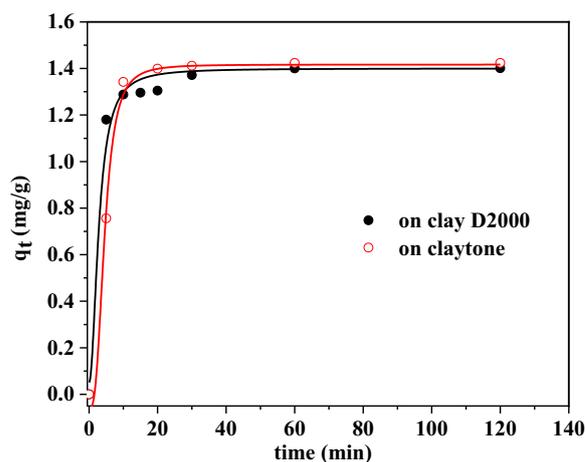

Fig. 3 Time profile of the adsorption equilibrium of MB onto claytone and clayD2000 (2 g/L) at 25 °C, $[MB]_0 = 239.5$ mg/L, pH = 2 for claytone and pH = 6 for clay D2000

Impact of contact time

Figure 3 presents the time profile of the adsorption equilibrium of MB onto claytone and clayD2000. The adsorption of MB was very rapid in the first 10 min, and then, as time passes, it steadily diminishes until it reaches equilibrium. The availability of more adsorption sites on the surface of the two adsorbents could explain the increase in adsorption activity at the initial state. Thereafter, the amount of MB dye adsorbed on both surfaces reduces as the adsorption rate falls, as a result, the equilibrium was attained. Under the experimental conditions, the amount of dye adsorbed at the equilibrium time ($q_e \approx 1.4$ mg g^{-1} for both surfaces) reflected the adsorbent's maximal

adsorption capacity. The contact time prerequisite to reach the equilibrium condition for MB on claytone and clayD2000 was about 60 min.

Adsorption kinetics

Several kinetic models were applied to assess the kinetic behavior of dye adsorption onto claytone and clayD2000. To calculate the rate constants and understand the process of adsorption, experimental data (which were collected in 3.2.1) were fitted into pseudo-first order, pseudo-second order, and intraparticle diffusion models. The equations of the three models are given in the supporting information Equs. (1, 2 and 3, respectively). The data acquired from the linear plots are recorded in Table 1. The pseudo-second-order kinetic model fits the experimental kinetic data with correlation coefficient (R^2) values close to unity for both surfaces, confirming typical

chemical adsorption [46], Turan et al. [53]). Lowered R^2 values of the pseudo-first-order model, suggest that this model failed to adequately describe the experimental data. The similar values of the experimental adsorption capacity at equilibrium ($q_{e,exp}$) and the estimated ($q_{e,cal}$) from the equation further support the great convention between the experimental data and pseudo-second order. Elsherbiny et al. have found that the second-order kinetic model was the best appropriate model for explaining the adsorption of MB on another modified montmorillonite [10].

Finally, the intraparticle diffusion model (Morris et al. [50]) was applied to the experimental data to study if the adsorption process is controlled only by intraparticle diffusion or if other phenomena such as surface adsorption, ion exchange, and complexation are involved (Bustos et al. [28]). The examination of Fig. S1 indicates that two intersected linear stages for the adsorption of MB on claytone and clayD2000 and the lines are not passing through the origin. It indicated that there are additional processes involved in the adsorption removal process than intraparticle diffusion and that intraparticle diffusion was not the rate-limiting step.

Adsorption isotherm

The equilibrium adsorption isotherms were investigated to better understand how MB interacts with the two surfaces and to compute the maximum adsorption capacity. In this study, the experimental adsorption data at equilibrium were matched with three models: Langmuir, Freundlich and Dubinin-Radushkevich (D-R) isotherm models. The equation and enlarged explanation of these models were given in the supporting information Equs. (4, 5 and 6, respectively). The data obtained from isotherm models are listed in Table 2. By comparing the correlation

Table 1 Kinetics data with their correlation coefficient (R^2) for the adsorption of MB onto claytone and clayD2000 at 25 °C

Model	Parameters	Adsorbents	
		Claytone	ClayD2000
Pseudo-first order	$q_{e,cal}$ (mg g^{-1})	9.853	0.593
	k_1 (min^{-1})	0.162	0.103
	R^2	0.881	0.947
Pseudo-second order	$q_{e,exp}$ (mg g^{-1})	1.424	1.401
	$q_{e,cal}$ (mg g^{-1})	1.453	1.416
	k_2 (g mg^{-1} min^{-1})	0.559	0.606
	R^2	0.998	0.999
Intra-particle diffusion	k_{p1} (mg g^{-1} min$^{-0.5}$)	0.271	0.053
	R^2	0.733	0.886
	k_{p2} (mg g^{-1} min$^{-0.5}$)	0.004	0.005
	R^2	0.732	0.695

Table 2 Isotherm parameters and the correlation coefficient, R^2 for the adsorption of MB dye onto claytone and clay D2000

Model	Parameters	Temperature/K					
		298		308		318	
		Claytone	CayD2000	Claytone	ClayD2000	Claytone	ClayD2000
Langmuir	q_{max} (mg g^{-1})	2.749	2.555	5.125	3.726	5.523	5.555
	K_L (L mg^{-1})	1.488	1.726	2.624	0.647	3.913	0.399
	R^2	0.987	0.997	0.918	0.981	0.959	0.911
Freundlich	n	2.762	3.344	1.6181	1.789	1.555	1.112
	K_F (mg g^{-1})	1.535	0.412	5.317	1.430	6.079	1.446
	R^2	0.829	0.868	0.959	0.872	0.981	0.970
D-R	q_m (mg g^{-1})	2.405	2.228	3.770	2.575	3.976	2.913
	$K_{D-R} \times 10^3$ (mol^2 k J^{-2})	− 0.1110	− 0.1736	− 0.0337	− 0.0921	− 0.0274	− 0.0642
	E (kJ/mol)	2.123	1.697	3.854	2.329	4.274	2.791
	R^2	0.9518	0.9598	0.9446	0.9823	0.9814	0.9575

Alkayal *et al. Environmental Sciences Europe*   (2023) 35:45

Page 6 of 11

coefficients (R^2), the adsorption of MB on claytone followed Langmuir isotherm at 298 K. At higher temperatures (308 and 318 K), the adsorption of MB on claytone obeyed Freundlich isotherm model with (n) values higher than unity, indicating the adsorption process was favorable (Aftab et al. [48]). The maximum adsorption capacity, q_{max} increased with increasing temperature, implying this adsorption may be an endothermic process. However, the adsorption of MB on clayD2000 was declared by Langmuir at a temperature of 298 and 308 K, by increasing the temperature to 318 K, the adsorption was supposed to predict multilayer as Freundlich isotherm. The intensity factor (n) declined with increasing temperature but is still higher than unity. The D-R model provides information about the mean sorption energy (E) which predicts the type of adsorption on the surface. The adsorption of MB on claytone and clayD2000 was governed by physical adsorption, since the value of (E) was < 8 kJ/mol. Moreover, the temperature has a positive effect on the values of (E) for both surfaces.

Influence of temperature and thermodynamic parameters

The influence of temperature on the adsorption of MB onto claytone and clayD2000 was studied at three different temperatures 295, 308 and 318 K. The impact of temperature on the adsorption process permits us to obtain thermodynamic parameters of adsorption such as ΔG°, ΔH°, and ΔS°. These thermodynamic parameters are evaluated using the Van't Hoff Eq. (2) [47] and Eq. (3) [34].

$$\ln \left(K_{Eq}^{\circ} \right) = \Delta S^{o}/R - \Delta H^{o}/RT \tag{2}$$

$$\Delta G^{o} = \Delta H^{o} - T \Delta S^{o} \tag{3}$$

where $K^{\circ}_{Eq} = (K_L C^0/\gamma_{adsorbate})$ is the standard thermodynamic equilibrium constant, K_L is Langmuir constant, C^0 is the standard concentration of adsorbate and equal 1 mol/L, $\gamma_{adsorbate}$ is the activity coefficient of adsorbate and can be negligible under dilute ionic solution [47]. T is the absolute temperature, and R is the gas constant.

The slope and intercept of Van't Hoff's plot (Figure not shown) were used to calculate the values of enthalpy change (ΔH°) and entropy change (ΔS°) (Table 3). The positive value of ΔH° (Table 3) of the adsorption of MB onto claytone displayed the endothermic behavior of the process. Additionally, its value is less than 40 kJ/mol confirming that the process is physisorption in nature [8]. However, ΔH° has a negative value in the case of adsorption of MB on clay2000 implying the process is chemosorption. Gibbs energy change for adsorption (ΔG°) has negative values for the adsorption of MB on claytone, showing that the adsorption process was thermodynamically favorable to take place [23]. The negative values decrease as temperature increases, indicating that the adsorption process was favorable at higher temperatures [34]. For the adsorption of MB on clay D2000, ΔG° has a negative value at 298 and it becomes positive at 308 K and 318 K, implying that the feasibility of the process decreased with raising the temperature. The positive value of ΔS° for the adsorption of MB on claytone revealed that increasing the randomness at the solution/adsorbent interface during the adsorption process [5]. For the uptake of MB by clayD2000, ΔS° had negative values revealing that the disorder at the solid–liquid interface was decreased [6].

Characterization of loaded clay/epoxy/nanocomposites
XRD

It was reported that the XRD pattern of intercalated Jeffamine/clay (clay D2000) displayed a d-spacing of 18.4 Å with an expansion of 9.1 Å due to the incorporation of two polymer layers or buckled structure of Jeffamine D-2000 [40]. For APA (claytone), a silicate reflection at 2θ of 4.8° corresponding to 18.4 Å was reported [39]. The characteristic peak to 001 plane of claytone and clayD2000 was shifted to 2θ value of 5.15° and 4.62°, respectively, after the adsorption of MB on them (see Fig. 4a). The shift of 2θ to a higher value in case of claytone after adsorption of MB indicating to contract in the interlayer spaces. This may be attributed to the exchanged and adsorbed MB or its molecular arrangement [10]. However, the decrease of 2θ value indicates

Table 3 Thermodynamic parameters of MB dye adsorbed onto claytone and clay D2000

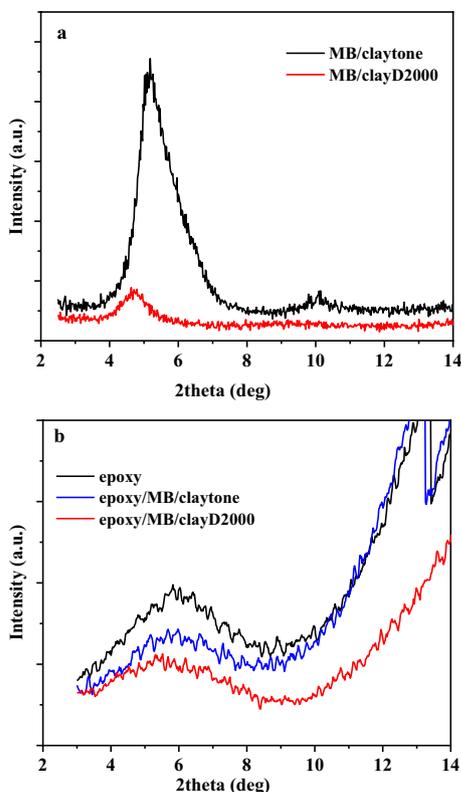| Adsorbent	Temp (K)	K^0_{Eq}	ΔH (kJmoL^{-1})	ΔG (kJmoL^{-1})	ΔS (JmoL^{-1} K^{-1})
Claytone	298	1.488		-1.038	131.5
	308	2.624	38.15	-2.352	
	318	3.913		-3.667	
CayD2000	298	1.726		-1.176	-190.3
	308	0.647	-57.89	0.727	
	318	0.399		2.63	

Fig. 4 XRD pattern of (**a**) adsorbed MB on claytone and clayD2000, (**b**) epoxy resin, epoxy/MB/claytone and epoxy/MB/clayD2000

the intercalation of MB between layers of clayD2000. For epoxy resin a broad peak at 2θ of 5.9° confirms the amorphous structure, Fig. 4b. The peak characteristic of epoxy resin was observed in epoxy/MB/clay nanocomposites however, the peak characteristic to 001 in claytone and clay D2000 after adsorption of MB at 2θ of 5.15° and 4.62° was not observed. This is attributed to the formation of exfoliated nanocomposites or blocking of d_{001} by the broad peak of epoxy. The exfoliation of the clay's layers was confirmed by TEM measurements.

TEM
To observe the dispersion state of MB/clay into epoxy resin, TEM micrographs were obtained for the nanocomposites. Figure 5 depicts the TEM of pristine epoxy (a), epoxy/MB/claytone/(b), and epoxy/MB/clayD2000 (c) with a clay ratio of 7.5 wt %. The TEM micrograph of epoxy resin shows a smooth featureless morphology. However, the nanocomposites revealed the dispersion of loaded clays (dark lines in the images with an average space between layers of 10 and 40 nm for MB/claytone and MB/clayD2000, respectively) into the epoxy matrix (bright lines). No aggregation of the clay's layers was noticed in TEM micrographs and this was confirmed by

XRD since exfoliated nanocomposites were formed. For the epoxy/MB/clayD2000 nanocomposite confirming the exfoliation of clay layers (red arrows). It is worth mentioning that the dark particles (blue arrows) observed in the micrograph may be due to the adsorbed dye MB on the clay surface.

TGA
TGA was used to assess the thermal behavior of the nanocomposites during the heating process as well as their thermal stability. The thermogram of epoxy resin displays one step of weight loss at 329.9 °C, Fig. 6. This single step corresponds to the resin decomposition without any release of any molecules during the heating process. The temperature at weight loss 10% (t10, °C), 50% (t50, °C) and 90% (t90, °C) of epoxy/MB/clayD2000 composite were improved from 362.9, 391.1, and 614.7 °C in pristine epoxy to 368.7, 404.5, and 775.6 °C, respectively, as appeared in Table 4. This behavior confirms that the addition of MB/clayD2000 improves the thermal properties of epoxy resin. The epoxy/MB/claytone nanocomposite tends to degrade slightly faster than the epoxy resin in the temperature range. However, the overall thermal resistance is still higher in colored epoxy due to the constrained region in the nanocomposite. Moreover, the char yield of epoxy/MB/claytone and epoxy/MB/clayD2000 nanocomposites was 5.14% and 9.66%, respectively, which is higher than that of bare epoxy (0.97%). The presence of dispersed exfoliated layered silicate acts as a barrier and increases the mean free path of decomposed molecules and delayed the decomposition temperature.

Hardness
The hardness test was carried out to examine the influence of the inclusion of modified clays loaded dye into the epoxy resin. The average values of the hardness of epoxy and the two prepared nanocomposites are listed in Table 4. The hardness of the epoxy resin was significantly improved despite the small amount of modified clays loaded dye which makes them especially attractive. Moreover, the epoxy/MB/clayD2000 nanocomposite had the highest hardness value.

Antimicrobial activity
The human pathogenic bacteria *Escherichia coli, Bacillus subtilis, Salmonella typhimurium, Klebsiella pneumoniae, Staphlococcus aureus,* and *Pseudomonas aeruginosa* as well as the yeast *Candida albicans* were not inhibited by the antimicrobial activity of the investigated nanocomposites epoxy/MB/claytone and epoxy/MB/clayD2000, Fig. 7. Whereas epoxy resin displayed distinct inhibition zones of according to the findings,
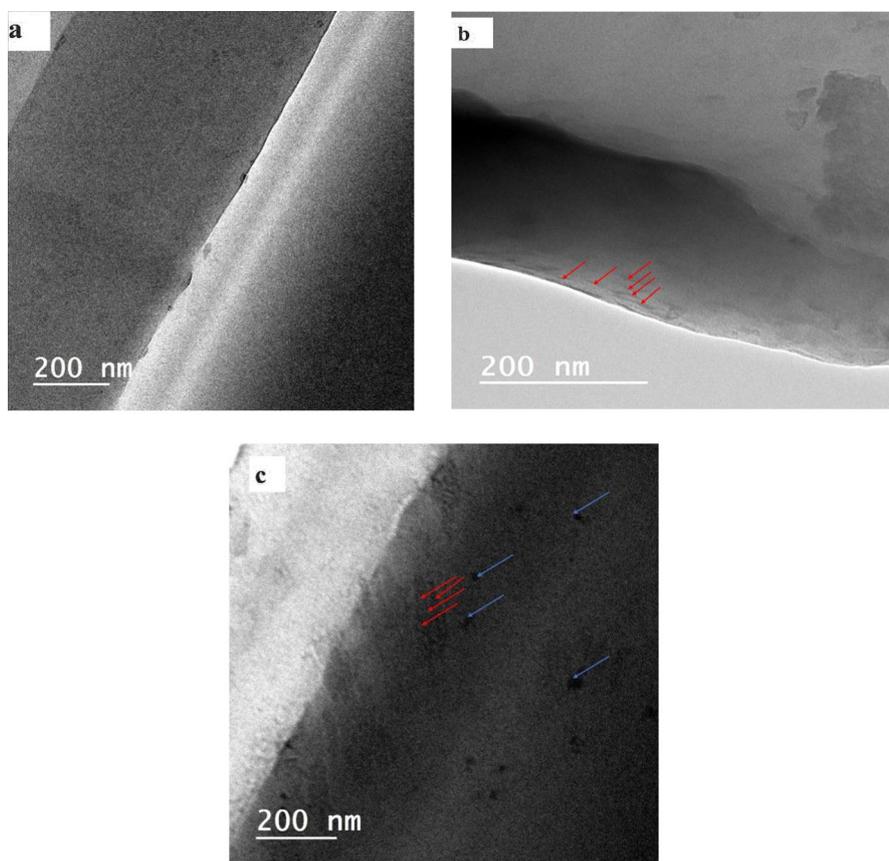
Alkayal *et al. Environmental Sciences Europe*   (2023) 35:45

Page 8 of 11

Fig. 5 TEM micrograph of **a** epoxy resin, **b** epoxy/MB/claytone, and **c** epoxy/MB/clayD2000
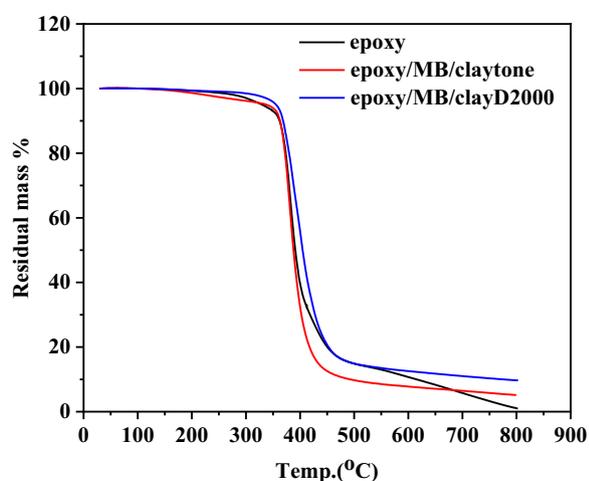

Fig. 6 TGA curve for epoxy resin, epoxy/MB/claytone, and epoxy/MB/clayD2000

Table 4 Thermal stability factors and average hardness of epoxy, epoxy/MB/claytone and epoxy/MB/clayD2000 nanocomposites

Sample code	t_{IDT} (°C)	t_{10} (°C)	t_{50} (°C)	t_{90} (°C)	Average hardness
Epoxy	337.7	362.9	391.1	614.7	27.00
Epoxy/MB/claytone	337.66	362.9	387.7	492.6	27.63
Epoxy/MB/clayD2000	355.31	368.7	404.5	775.6	31.20

differently. It is partially understood how epoxy resin inhibits the growth of germs. Cellular proteins supposedly become inactive, and DNA is thought to lose its replication capacity [11]. Moreover, it was demonstrated that epoxy attaches to protein functional groups, causing denaturation of the protein. Additionally, it drastically alters the bacterial membrane, making it impossible for the bacteria to correctly control transport through the plasma membrane, ultimately leading to cell death [43]. The synthesized nanocomposites epoxy/MB/claytone and epoxy/MB/clayD2000 have a hard surface, complex structure, and insoluble properties so, they have no permeability through cell structure and do not affect on the

the epoxy exhibited good antibacterial and antifungal activities of varied intensities, Fig. 8. This might be because the epoxy resin and the tested organisms interact
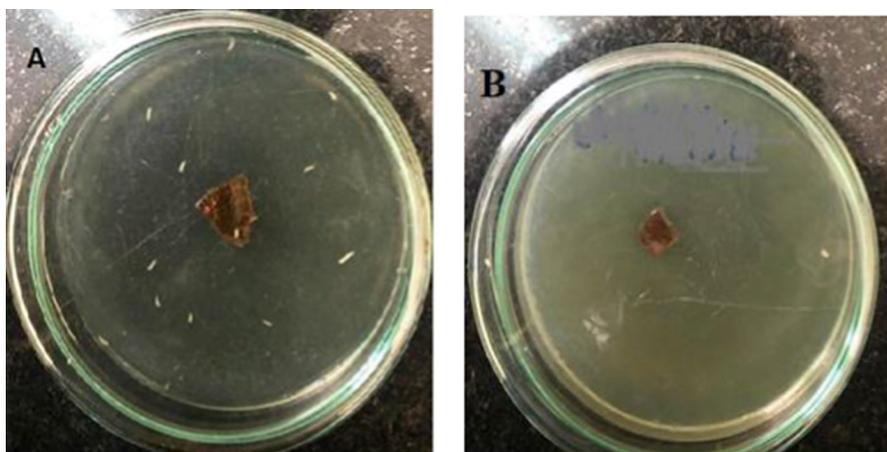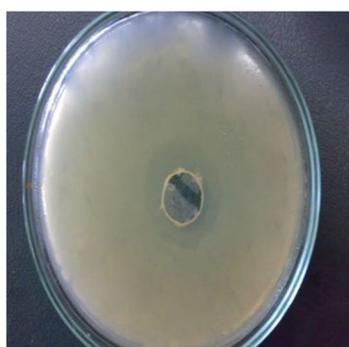
Fig. 7 Antimicrobial activity of (**A**) epoxy/MB/claytone and (**B**) epoxy/MB/clayD2000
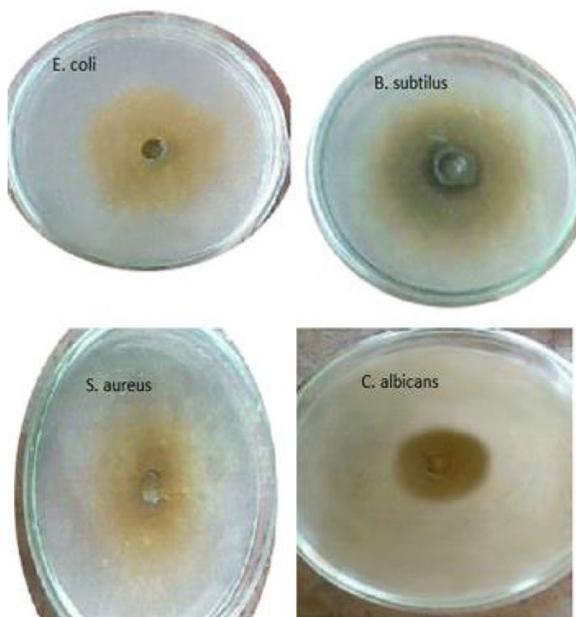

Control

Fig. 8 Antimicrobial activity of epoxy resin against different pathogenic organisms

microbial growth. Also, microorganisms cannot secrete any enzymes to degrade the previous nanocomposites (epoxy/MB/claytone and epoxy/MB/clayD2000) and cannot absorb this nanocomposite.

Conclusion

Two modified montmorillonites namely, claytone and clayD2000 were used to remove methyl blue as a model of anionic dye from an aqueous solution by adsorption process. The maximum adsorption efficiency of claytone was found in an acidic medium, however, clayD2000 in neutral within 60 min. Pseudo-second-order kinetic model was the most appropriate model for explaining the adsorption of MB on both surfaces. The adsorption of MB on claytone and clayD2000 followed Langmuir isotherm at lower temperature and with increasing the temperature was supposed to predict multilayer as Freundlich isotherm. The enthalpy change ($\Delta H°$), and Gibbs energy change ($\Delta G°$) showed that the adsorption process MB on claytone was a favorable and endothermic process. However, an exothermic behavior for the uptake of MB by clayD2000 and a favorable process at lower temperatures. In a sustainable step, the colored clays that had been loaded with MB dyes were incorporated into epoxy resin to prepare fashionable layered polymer nanocomposites. TEM results demonstrated that the loaded clays were dispersed into the epoxy matrix. The large distance between clays' lines in TEM images confirms the exfoliation of clay layers as confirmed by XRD. TGA results confirmed that the addition of MB/clayD2000 improves the thermal properties of epoxy resin. For epoxy /MB/claytone nanocomposite, it degraded slightly faster than the epoxy resin in the temperature range. However, the overall thermal resistance is still higher in colored epoxy due to the constrained region in the nanocomposite. The

hardness of the epoxy resin was significantly improved despite the small amount of modified clays loaded dye. The epoxy/MB/clayD2000 nanocomposite had the highest hardness value. The human pathogenic bacteria *E. coli, B. subtilis, S. typhimurium, K. pneumoniae, St. aureus, P. aeruginosa*, and the yeast-like fungus *C. albicans* did not respond to epoxy/MB/claytone or epoxy/MB/clayD2000.

Supplementary Information

> **Additional file 1: Fig. S1**. Intraparticle diffusion plot of adsorption of MB on claytone and clayD2000.

Author contributions
NSA, ASE, SEE, and NAS: validation; NSA, ASE, SEE, and NAS: formal analysis; ASE, SobhyEE, and NAS: investigation and data curation; NSA, ASE, SEE: writing-original draft preparation; ASE, NAS: review and editing; ASE, NAS; Put the idea of the work and final revision. All authors read and approved the final manuscript.

Availability of data and materials
All the data are introduced in the manuscript.

Declarations

Ethics approval and consent to participate
Not applicable.

Consent for publication
All authors agree to publish the prepared paper in Environmental Science Europe.

Competing interests
The authors declare no conflict of interest.

References
1. Apler A, Snowball I, Frogner-Kockum P, Josefsson S (2019) Distribution and dispersal of metals in contaminated fibrous sediments of industrial origin. Chemosphere 215:470–481
2. Bergaya F, Lagaly G (2013) Handbook of clay science. Newnes, Oxford
3. Brown, G. (1982). Crystal structures of clay minerals and their X-ray identification, The Mineralogical Society of Great Britain and Ireland
4. Chung K-T (2016) Azo dyes and human health: a review. J Environ Sci Health C 34(4):233–261
5. Çınar S, Kaynar ÜH, Aydemir T, Kaynar SC, Ayvacıklı M (2017) An efficient removal of RB5 from aqueous solution by adsorption onto nano-ZnO/Chitosan composite beads. Int J Biol Macromol 96:459–465
6. Dang YT, Dang M-HD, Mai NXD, Nguyen LHT, Phan TB, Le HV, Doan TLH (2020) Room temperature synthesis of biocompatible nano Zn-MOF for the rapid and selective adsorption of curcumin. J Sci Adv Mater Dev 5(4):560–565
7. De Paiva LB, Morales AR, Díaz FRV (2008) Organoclays: properties, preparation and applications. Appl Clay Sci 42(1–2):8–24
8. El-Hamshary H, Elsherbiny AS, El-Newehy MH, El-Hefnawy ME (2020) Polyaspartate-Ionene/Na+-Montmorillonite nanocomposites as novel adsorbent for anionic dye; effect of ionene structure. Polymers 12(12):2843
9. Elsherbiny AS (2013) Adsorption kinetics and mechanism of acid dye onto montmorillonite from aqueous solutions: stopped-flow measurements. Appl Clay Sci 83:56–62
10. Elsherbiny AS, El-Hefnawy ME, Gemeay AH (2017) Linker impact on the adsorption capacity of polyaspartate/montmorillonite composites towards methyl blue removal. Chem Eng J 315:142–151
11. Feng QL, Wu J, Chen GQ, Cui F, Kim T, Kim J (2000) A mechanistic study of the antibacterial effect of silver ions on *Escherichia coli* and *Staphylococcus aureus*. J Biomed Mater Res 52(4):662–668
12. Ferguson LR, Baguley BC (1988) Verapamil as a co-mutagen in the Salmonella/mammalian microsome mutagenicity test. Mutat Res Lett 209(1–2):57–62
13. Godiya CB, Cheng X, Deng G, Li D, Lu X (2019) Silk fibroin/polyethylenimine functional hydrogel for metal ion adsorption and upcycling utilization. J Environ Chem Eng 7(1):102806
14. Godiya CB, Xiao Y, Lu X (2020) Amine functionalized sodium alginate hydrogel for efficient and rapid removal of methyl blue in water. Int J Biol Macromol 144:671–681
15. Ho M-W, Lam C-K, Lau K-T, Ng DH, Hui D (2006) Mechanical properties of epoxy-based composites using nanoclays. Compos Struct 75(1–4):415–421
16. Holme, I. (1984). Ecological Aspects of Colour Chemistry in Developments in the Chemistry and Technology of Organic Dyes. Ed. J. Griffiths, Pub. Soc. Chem. & Ind 111
17. Islam M, Parimalam M, Sumdani M, Taher M, Asyadi F, Yenn T (2020) Rheological and antimicrobial properties of epoxy-based hybrid nanocoatings. Polym Testing 81:106202
18. Jia J, Sun X, Lin X, Shen X, Mai Y-W, Kim J-K (2014) Exceptional electrical conductivity and fracture resistance of 3D interconnected graphene foam/epoxy composites. ACS Nano 8(6):5774–5783
19. Konicki W, Hełminiak A, Arabczyk W, Mijowska E (2018) Adsorption of cationic dyes onto Fe@ graphite core–shell magnetic nanocomposite: Equilibrium, kinetics and thermodynamics. Chem Eng Res Des 129:259–270
20. Wang L, Wang K, Chen L, Zhang Y, He C (2006) Preparation, morphology and thermal/mechanical properties of epoxy/nanoclay composite. Compos Part A 37:1890–1896
21. Lim JY, Goh SS, Liow SS, Xue K, Loh XJ (2019) Molecular gel sorbent materials for environmental remediation and wastewater treatment. J Mater Chem A 7(32):18759–18791
22. Lim SH, Gürsoy NÇ, Hauser P, Hinks D (2004) Performance of a new cationic bleach activator on a hydrogen peroxide bleaching system. Color Technol 120(3):114–118
23. Lima EC, Hosseini-Bandegharaei A, Moreno-Piraján JC, Anastopoulos I (2019) A critical review of the estimation of the thermodynamic parameters on adsorption equilibria. Wrong use of equilibrium constant in the Van't Hoof equation for calculation of thermodynamic parameters of adsorption. J Mol Liq 273:425–434
24. Mark A (2008) Science and technology for water purification in the coming decades. Nature 452:20
25. Mogale R, Akpomie KG, Conradie J, Langner EHG (2022) Dye adsorption of aluminium- and zirconium-based metal organic frameworks with azobenzene dicarboxylate linkers. J Environ Manage 304:114166
26. Murray KE, Thomas SM, Bodour AA (2010) Prioritizing research for trace pollutants and emerging contaminants in the freshwater environment. Environ Pollut 158(12):3462–3471
27. Murugesan A, Divakaran M, Raveendran P, Nitin Nikamanth A, Thelly KJ (2019) An eco-friendly porous poly (imide-ether) s for the efficient removal of methylene blue: adsorption kinetics, isotherm, thermodynamics and reuse performances. J Polym Environ 27(5):1007–1024
28. Ndiaye B, Bustos G, Calvar S, Vecino X, Cruz JM, Moldes AB, Pérez-Cid B (2019) Selective adsorption capacity of grape marc hydrogel for

Alkayal *et al. Environmental Sciences Europe*   (2023) 35:45

Page 11 of 11

adsorption of binary mixtures of dyes. Water Air Soil Pollut. https://doi.org/10.1007/s11270-019-4358-8

29. Parimalam M, Islam MR, Yunus RM (2018) Effects of nanosilica, zinc oxide, titatinum oxide on the performance of epoxy hybrid nanocoating in presence of rubber latex. Polym Testing 70:197–207

30. Parimalam M, Islam MR, Yunus RM (2019) Effects of nano-and micro-sized inorganic filers on the performance of epoxy hybrid nanocoatings. Polym Polym Compos 27(2):82–91

31. Parimalam M, Islam MR, Yunus RM (2019) Effects of nanosilica and titanium oxide on the performance of epoxy–amine nanocoatings. J Appl Polym Sci 136(35):47901

32. Park YJ, Fray DJ (2009) Recovery of high purity precious metals from printed circuit boards. J Hazard Mater 164(2–3):1152–1158

33. Pridham T, P. Anderson, C. Foley L. Lindenfelser, C. Hesseltine and R. Benedict (1957). A selection of media for maintenance and taxonomic study of streptomycetes. A selection of media for maintenance and taxonomic study of streptomycetes

34. Purkait M, Gusain D, DasGupta S, De S (2005) Adsorption behavior of chrysoidine dye on activated charcoal and its regeneration characteristics by using different surfactants. Sep Sci Technol 39(10):2419–2440

35. Razi Z, Islam M, Parimalam M (2019) Mechanical, structural, thermal and morphological properties of a protein (fish scale)-based bisphenol-A composites. Polym Testing 74:7–13

36. Richardson SD, Kimura SY (2016) Water analysis: emerging contaminants and current issues. Anal Chem 88(1):546–582

37. Sabnis RW (2010) Handbook of biological dyes and stains: synthesis and industrial applications. John Wiley & Sons, Hoboken

38. Sahnoun S, Boutahala M (2018) Adsorption removal of tartrazine by chitosan/polyaniline composite: kinetics and equilibrium studies. Int J Biol Macromol 114:1345–1353

39. Salahuddin N, Moet A, Hiltner A, Baer E (2002) Nanoscale highly filled epoxy nanocomposite. Eur Polymer J 38(7):1477–1482

40. Salahuddin NA (2004) Layered silicate/epoxy nanocomposites: synthesis, characterization and properties. Polym Adv Technol 15(5):251–259

41. Shi X, Tian A, You J, Yang H, Wang Y, Xue X (2018) Degradation of organic dyes by a new heterogeneous Fenton reagent-Fe2GeS4 nanoparticle. J Hazard Mater 353:182–189

42. Siyar R, Ardejani FD, Farahbakhsh M, Norouzi P, Yavarzadeh M, Maghsoudy S (2020) Potential of Vetiver grass for the phytoremediation of a real multi-contaminated soil, assisted by electrokinetic. Chemosphere 246:125802

43. Sondi I, Matijević E (2003) Homogeneous precipitation by enzyme-catalyzed reactions. 2. Strontium and barium carbonates. Chem Mater 15(6):1322–1326

44. Song SH, Park KH, Kim BH, Choi YW, Jun GH, Lee DJ, Kong BS, Paik KW, Jeon S (2013) Enhanced thermal conductivity of epoxy–graphene composites by using non-oxidized graphene flakes with non-covalent functionalization. Adv Mater 25(5):732–737

45. Sumdani MG, Islam MR, Yahaya ANA (2019) The effects of anionic surfactant on the mechanical, thermal, structure and morphological properties of epoxy–MWCNT composites. Polym Bull 76:5919–5938

46. Tan Y, Chen M, Hao Y (2012) High efficient removal of Pb (II) by amino-functionalized Fe3O4 magnetic nano-particles. Chem Eng J 191:104–111

47. Tran HN (2022) Improper estimation of thermodynamic parameters in adsorption studies with distribution coefficient KD (qe/Ce) or Freundlich constant (KF): considerations from the derivation of dimensionless thermodynamic equilibrium constant and suggestions. Adsorpt Sci Technol. https://doi.org/10.1155/2022/5553212

48. Usman M, Aftab R, Zaidi S, Adnan S, Rao R (2021) Adsorption of aniline blue dye on activated pomegranate peel: equilibrium, kinetics, thermodynamics and support vector regression modelling. Int J Environ Sci Technol. https://doi.org/10.1007/s13762-021-03571-0

49. Vickers NJ (2017) Animal communication: when i'm calling you, will you answer too? Curr Biol 27(14):R713–R715

50. Weber WJ Jr, Morris JC, Stumm W (1962) Determination of alkylbenzenesulfonates by ultraviolet spectrophotometry. Anal Chem 34(13):1844–1845

51. Wu S, Guo Q, Peng S, Hameed N, Kraska M, Stühn B, Mai Y-W (2012) Toughening epoxy thermosets with block ionomer complexes: a nanostructure–mechanical property correlation. Macromolecules 45(9):3829–3840

52. Xu X, Jia Y, Xiao L, Wu Z (2018) Strong vibration-catalysis of ZnO nanorods for dye wastewater decolorization via piezo-electro-chemical coupling. Chemosphere 193:1143–1148

53. Yılmazoğlu M, Turan B, Demircivi P, Hızal J (2022) Synthesis and characterization of imidazolium based ionic liquid modified montmorillonite for the adsorption of Orange II dye: effect of chain length. J Mol Struct. https://doi.org/10.1016/j.molstruc.2021.131628

54. Zhou CH, Keeling J (2013) Fundamental and applied research on clay minerals: From climate and environment to nanotechnology. Appl Clay Sci 74:3–9

Publisher's Note